

Supporting Information

An Excellent Benzocoumarin-based Ratiometric Two-Photon Fluorescent Probe for H₂O₂

Xue-Li Hao,^a Zi-Jing Guo,^b Chun Zhang,^a and Ai-Min Ren,*^a

^a Laboratory of Theoretical and Computational Chemistry, Institute of Theoretical Chemistry, Jilin University,
Liutiao Road 2#, Changchun 130061

^b School of Optoelectronics, Beijing Institute of Technology, Beijing 100081, People's Republic of China

*Corresponding author: Ai-Min Ren

Tel.: +86 431 88498961; Fax: +86 431 88945942;

E-mail addresses: aimin_ren@yahoo.com

Table of Contents

1. The theoretical basis of fluorescence quantum yield.
2. The theoretical basis of two-photon absorption cross section.
3. Figure S1. Geometrical structures and corresponding names of the isomeric molecules.
4. Figure S2. Contour surfaces of the frontier molecular orbitals for fluorescent isomeric molecules.
5. Figure S3. Contour surfaces of the frontier molecular orbitals for fluorescent probe molecules (BC, BC-2, BC-3 and BC-4).
6. Figure S4. One-photon absorption and fluorescence spectra of the studied molecules in gas, toluene, chloroform (CHCl_3), methanol (MeOH), dimethylsulfoxide (DMSO) and water.
7. Figure S5. Structures and corresponding names of experimental molecules
8. Table S1. Calculated vertical excitation energies (Evt), maximum absorption peaks (λ_{abs}), and the corresponding oscillator strengths (f) at the ground-state geometries of experimental molecules (DCCA, DCCA-Me (4) and 2-Me (6)) in water by TD-DFT method using different functionals.
9. Table S2. Calculated vertical excitation energies (Evt), emission peaks (λ_{ems}), and the corresponding oscillator strengths (f) at the exited-state geometries of experimental molecules (DCCA, DCCA-Me (4) and 2-Me (6)) in water by TD-DFT method using different functionals.
10. Table S3. Calculated OPA properties including maximum absorption peaks (λ_{abs}), vertical excitation energies (ω_0f), oscillator strengths (f), transition moments (μ_0f) and corresponding transition nature of the all molecules by B3LYP/6-311+G (d) method in water solvent.
11. Table S4. Fluorescence properties including maximum emission peaks (λ_{em}), oscillator strengths (f), fluorescence lifetimes (τ) and transition nature of the all molecules calculated by TDDFT method in water.
12. Table S5. Calculated the maximum two-photon absorption cross sections (σ_{max})

and corresponding TPA wavelengths (λ_{max}), at the ground-state geometries of experimental molecules (DCCA and CMg1) by TD-DFT /6-311+G (d) methods, using different functionals.

13. Figure S6. Structures of fluorescent probe molecules and the divided regions for NBO analysis
14. Table S6. Natural atomic orbital occupancies analysis for fluorescent probe molecules.
15. Fig.S7. Molecular structures and reactive site atoms for fluorescent probe molecules
16. Table S7. NBO analysis for fluorescent probe molecules at the ground state S0 and the first excited state S1.

The Fluorescence Quantum Yield

The fluorescence quantum yield is an important index for fluorescent probes and it can be expressed as:

$$\Phi = \frac{k_r}{k_r + k_{nr}} \quad (4)$$

There, the k_r and k_{nr} are respective the radiative and nonradiative decay rate, and nonradiative decay rate includes internal conversion rate and intersystem crossing rate.

As can be seen, the spontaneous emission rate(k_r)is the integration of the emission spectrum: ¹

$$k_r = \int_0^{\infty} \sigma_{em}(\omega) d\omega \quad (5)$$

according to Fermi's golden rule, the $\sigma_{em}(\omega)$ can be expressed as:²

$$\sigma_{em}(\omega) = \frac{4\omega^3}{3c^3} \sum_{v_i, v_f} P_{iv_i}(T) \left| \langle \Theta_{fv_f} | \overset{\omega}{\mu} | \Theta_{iv_i} \rangle \right|^2 \delta(E_{if} + E_{iv_i} - E_{fv_f} - \hbar\omega) \quad (6)$$

Here, $\sigma_{em}(\omega)$ is defined as the rate of spontaneous photon emission per unit frequency between ω and $\omega+d\omega$ for per molecule. $P_{iv_i}(T)$ is the Boltzman distribution function for initial vibronic state and c is the velocity of light. The electric transition dipole moment can be expressed as $\overset{\omega}{\mu}_{fi} = \langle \Phi_f | \overset{\omega}{\mu} | \Phi_i \rangle$. According to the Born-Oppenheimer approximation, the initial wave function $|\Psi_{iv_i}\rangle = |\Phi_i \Theta_{iv_i}\rangle$ can be described by the products of the electronic states $|\Phi_i\rangle$ and the vibrational states $|\Theta_{iv_i}\rangle$. The same description can be seen in the final wave function. Addition to, E_{if} is the difference of adiabatic energy between two states, while E_{iv_i} and E_{fv_f} are the vibrational energies in the corresponding electronic states. Under the Franck-Condon approximation, the

$\sigma_{em}(\omega)$ can be defined as $\sigma_{em}^{FC}(\omega)$, and the delta function can be Fourier transformed

as:

$$\sigma_{em}^{FC}(\omega) = \frac{2\omega^3}{3\pi\hbar c^3} |\mu_0|^2 \int_{-\infty}^{+\infty} e^{-i(\omega-\omega_f)t} Z_{iv}^{-1} \rho_{em,0}^{FC}(t, T) dt \quad (7)$$

Where, Z_{iv}^{-1} is the partition function and $\rho_{em,0}^{FC}(t, T)$ is the thermal vibration correlation Function.^{1, 3}

The internal conversion rate (k_{ic}) can be defined as:⁴

$$k_{ic} = \frac{2\pi}{\hbar} |H'_{fi}|^2 \delta(E_{fi} + E_{fv_f} - E_{iv_i}) \quad (8)$$

and the non-Born-Oppenheimer coupling can be expressed as:⁵

$$H'_{fi} = -\hbar^2 \sum_l \left\langle \Phi_f \Theta_{fv_f} \left| \frac{\partial \Phi_i}{\partial Q_{fl}} \frac{\partial \Theta_{iv_i}}{\partial Q_{fl}} \right. \right\rangle \quad (9)$$

Applying the Condon approximation, the eq (9) can be described as:³

$$H'_{fi} = \sum_l \left\langle \Phi_f \left| \mathbf{P}_{fl} \right| \Phi_i \right\rangle \left\langle \Theta_{fv_f} \left| \mathbf{P}_{fl} \right| \Theta_{iv_i} \right\rangle \quad (10)$$

Inserting eq (10) into (8) and the delta function is Fourier transformed, the IC rate (k_{ic}) is expressed as:¹

$$k_{ic,kl} = \frac{1}{\hbar^2} R_{kl} \int_{-\infty}^{+\infty} e^{i\omega_f t} Z_{iv}^{-1} \rho_{ic,kl}(t, T) dt \quad (11)$$

Here, $R_{kl} = \left\langle \Phi_f \left| \mathbf{P}_{jk} \right| \Phi_i \right\rangle \left\langle \Phi_i \left| \mathbf{P}_{jl} \right| \Phi_f \right\rangle$ (12) The definition of Z_{iv}^{-1} and $\rho_{ic,kl}(t, T)$ is similar to the description above.

The two-photon absorption cross section

The two-photon absorption (TPA) cross section (σ^{TPA}) is an important index for evaluating the quality of two-photon fluorescent probes, which can be obtained from the two-photon transition probability ($\delta_{a.u}$) using:⁶

$$\sigma^{\text{TPA}} = \frac{4\pi^2 \alpha a_0^5 \omega^2}{15c\Gamma} \delta_{a.u} \quad (1)$$

Here, α , a_0 , ω and c are the fine structure constant, the Bohr radius, photon energy and the speed of light, respectively. Γ is the broadening factor describing the spectral broadening, which is assumed to be 0.05eV in order to make the theoretical simulation process consistent with the experimental spectra.⁷ The two-photon transition probability ($\delta_{a.u}$) is defined as:⁸

$$\delta_{a.u} = \frac{1}{30} \sum_{ab} (FS_{aa}\bar{S}_{bb} + GS_{ab}\bar{S}_{ab} + HS_{ab}\bar{S}_{ba}) \quad (2)$$

There, $a, b \in \{x, y, z\}$. For linearly polarized light with parallel polarization, the value F , H and G are 2, 2 and 2. For the circular case, they are -2, 3 and 2, respectively. In the electric dipole approximation, the two-photon transition moment matrix elements S_{ab}^{if} is expressed as:^{6b}

$$S_{ab}^{if}(\omega_1, \omega_2) = \frac{1}{\hbar} \sum_{n \neq i} \left\{ \frac{\langle i | \mu_a | n \rangle \langle n | \bar{\mu}_b | f \rangle}{\omega_{ni} - \omega_1} + \frac{\langle i | \mu_b | n \rangle \langle n | \bar{\mu}_a | f \rangle}{\omega_{ni} - \omega_2} \right\} \quad (3)$$

Here, i and f is the representation of the initial and final state, and n is one of a possible intermediate states. ω_{in} is excitation energy. ω_1, ω_2 are the energies of the two photons. $\langle i | \mu_a | n \rangle$ is the a 'th component of the transition dipole moment. These TPA parameters can be calculated using quadratic response theory by DALTON program.⁹

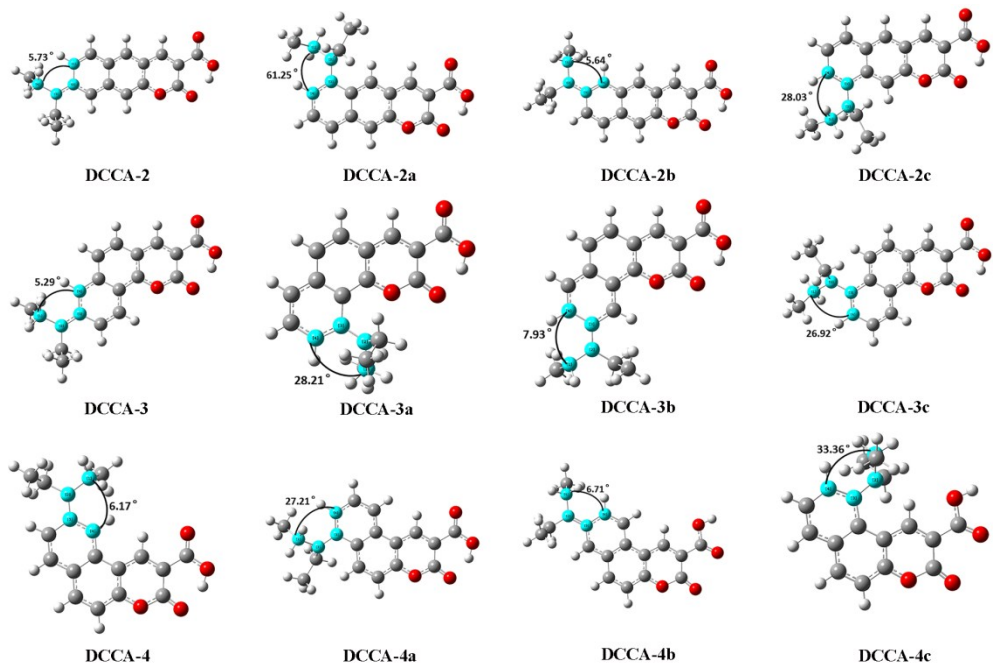


Fig.S1. Geometrical structures and corresponding names of the isomeric molecules

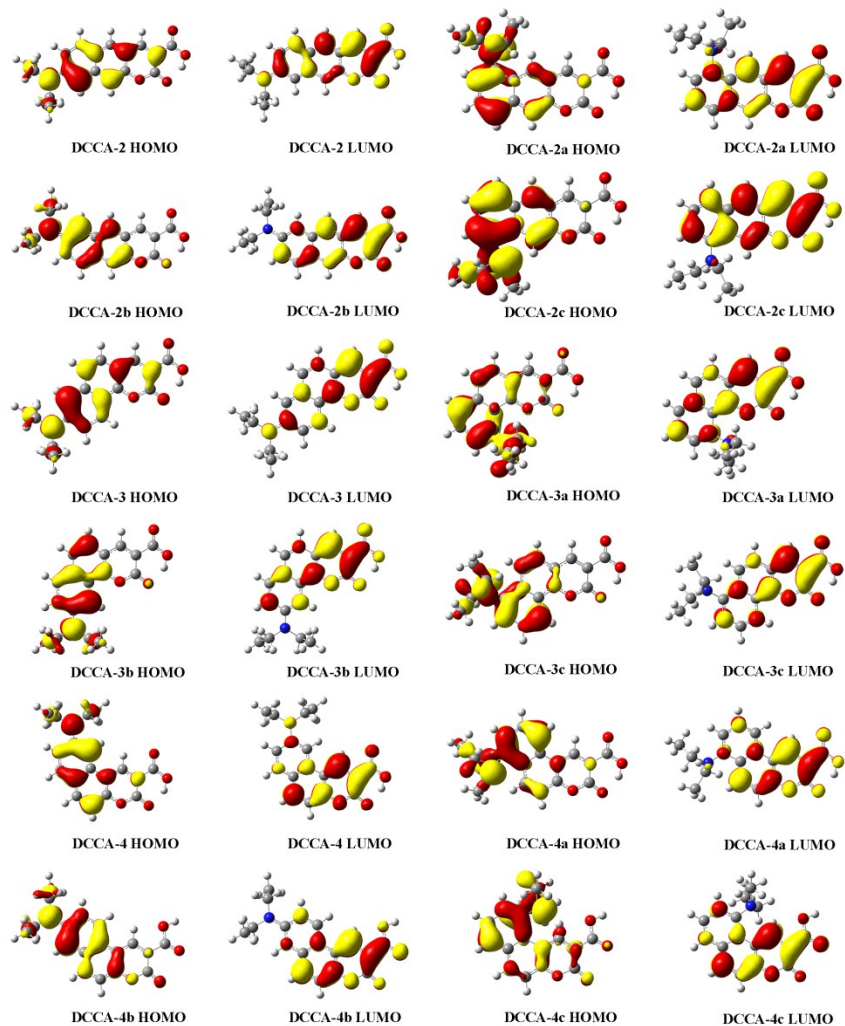


Fig.S2. Contour surfaces of the frontier molecular orbitals for fluorescent isomeric molecules

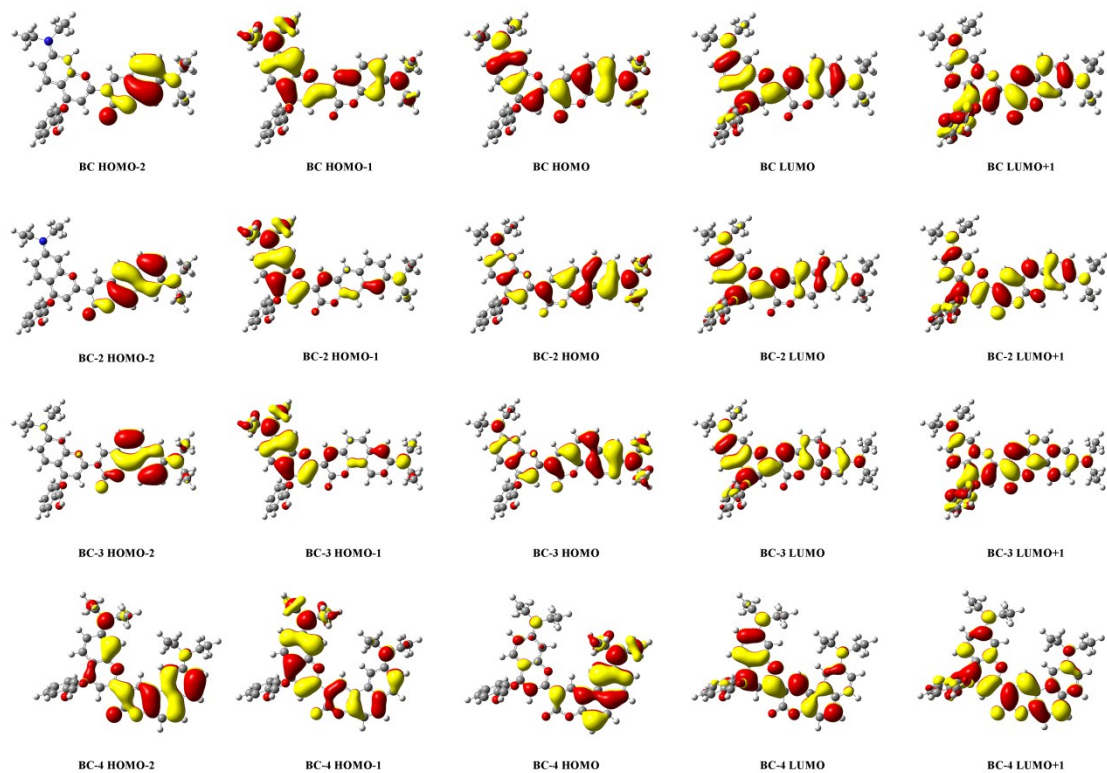


Fig.S3. Contour surfaces of the frontier molecular orbitals for fluorescent probe molecules (BC, BC-2, BC-3 and BC-4)

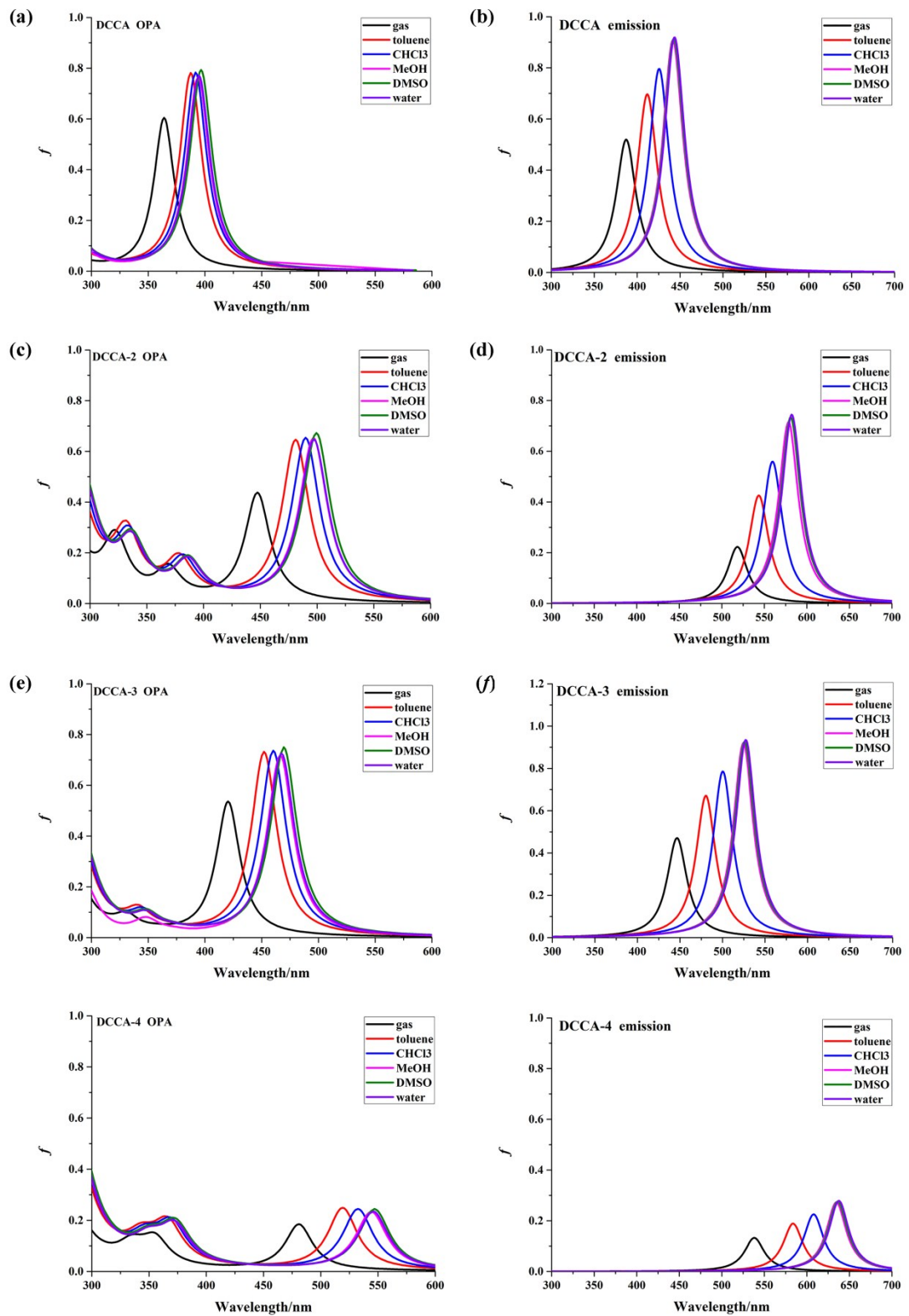
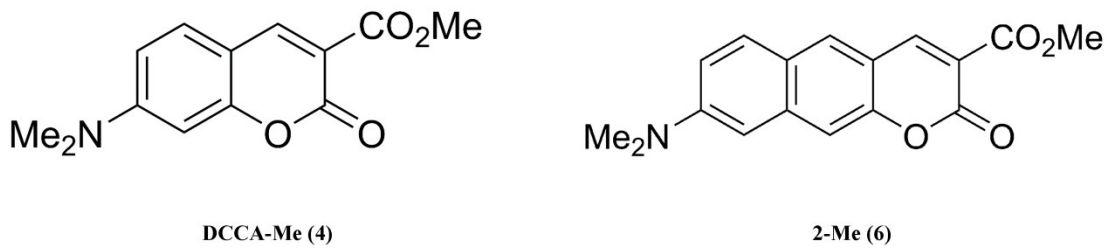


Fig.S4. One-photon absorption and fluorescence spectra of the studied molecules in gas, toluene, chloroform (CHCl₃), methanol (MeOH), dimethylsulfoxide (DMSO) and water



DCCA-Me (4)

2-Me (6)

Fig.S5. Structures and corresponding names of experimental molecules¹⁰

Table S1. Calculated vertical excitation energies (Evt), maximum absorption peaks (λ_{abs}), and the corresponding oscillator strengths (f) at the ground-state geometries of experimental molecules^{10, 11} (DCCA, DCCA-Me (4) and 2-Me (6)) in water by TD-DFT method using different functionals

molecule	functional	B3LYP	CAM-B3LYP	wB97XD	M062X	Experimental data
	HF%	20	19, 65	22.2, 100	54	
DCCA	Evt/eV	3.14	3.44	3.47	4.07	
	λ_{abs}/nm	395	360	357	305	411
	f	0.77	0.88	0.87	1.02	
DCCA-Me (4)	Evt/eV	3.20				
	λ_{abs}/nm	387				405
	f	0.79				
2-Me (6)	Evt/eV	2.58				
	λ_{abs}/nm	480				460
	f	0.62				

Table S2. Calculated vertical excitation energies (Evt), emission peaks (λ_{ems}), and the corresponding oscillator strengths (f) at the excited-state geometries of experimental molecules^{10, 11} (DCCA, DCCA-Me (4) and 2-Me (6)) in water by TD-DFT method using different functionals

molecule	functional	B3LYP	CAM-B3LYP	wB97XD	M062X	Experimental data
	HF%	20	19, 65	22.2, 100	54	
DCCA	Evt/eV	2.80	3.05	3.06	3.61	
	λ_{ems}/nm	444	406	405	343	472
	f	0.92	1.11	1.11	1.30	
DCCA-Me (4)	Evt/eV	2.87				
	λ_{ems}/nm	432				475
	f	0.98				
2-Me (6)	Evt/eV	2.21				
	λ_{ems}/nm	562				612

<i>f</i>	0.74
----------	------

Table S3. Calculated OPA properties including maximum absorption peaks (λ_{abs}), vertical excitation energies (ω_{0f}), oscillator strengths (f), transition moments (μ_{0f}) and corresponding transition nature of the all molecules by B3LYP/6-311+G(d) method in water solvent. The absorption wavelengths (λ^{exp}) are experimental results¹¹.

Molecule	λ^{exp}/nm	λ_{abs}^o/nm	ω_{0f}/eV	<i>f</i>	μ_{0f}/D	Transition nature	
DCCA	411	394.63	3.14	0.77	3.15	$S_0 \rightarrow S_1$	$H \rightarrow L$ (98.11%)
DCCA-2		497.23	2.49	0.64	3.23	$S_0 \rightarrow S_1$	$H \rightarrow L$ (96.18%)
		386.39	3.21	0.14	1.31	$S_0 \rightarrow S_2$	$H-1 \rightarrow L$ (88.42%)
		336.35	3.69	0.19	1.46	$S_0 \rightarrow S_3$	$H \rightarrow L+1$ (88.49%)
DCCA-3		467.36	2.65	0.72	3.33	$S_0 \rightarrow S_1$	$H \rightarrow L$ (97.90%)
		348.29	3.56	0.06	0.80	$S_0 \rightarrow S_3$	$H \rightarrow L+1$ (78.81%)
DCCA-4		545.79	2.27	0.23	2.02	$S_0 \rightarrow S_1$	$H \rightarrow L$ (99.17%)
		372.54	3.33	0.14	1.31	$S_0 \rightarrow S_2$	$H-1 \rightarrow L$ (94.10%)
BC		646	567.23	2.19	1.22	4.77	$S_0 \rightarrow S_1$ $H \rightarrow L$ (98.81%)
			455.49	2.72	0.13	1.37	$S_0 \rightarrow S_2$ $H-1 \rightarrow L$ (92.24%)
			377.64	3.28	0.16	1.42	$S_0 \rightarrow S_3$ $H \rightarrow L+1$ (62.92%)
BC-2			651.48	1.90	1.26	5.20	$S_0 \rightarrow S_1$ $H \rightarrow L$ (98.49%)
			501.69	2.47	0.13	1.46	$S_0 \rightarrow S_2$ $H-1 \rightarrow L$ (89.79%)
			428.04	2.90	0.20	1.66	$S_0 \rightarrow S_4$ $H \rightarrow L+1$ (90.58%)
BC-3			318.28	3.90	0.34	1.90	$S_0 \rightarrow S_{13}$ $H-2 \rightarrow L+1$ (57.23%)
							$H \rightarrow L+3$ (27.28%)
			636.56	1.95	1.29	5.21	$S_0 \rightarrow S_1$ $H \rightarrow L$ (98.55%)
			492.79	2.52	0.10	1.26	$S_0 \rightarrow S_2$ $H-1 \rightarrow L$ (93.26%)
			407.74	3.04	0.18	1.57	$S_0 \rightarrow S_4$ $H \rightarrow L+1$ (67.57%)
BC-4			365.65	3.39	0.14	1.30	$S_0 \rightarrow S_6$ $H-3 \rightarrow L$ (85.28%)
			720.38	1.72	0.35	2.87	$S_0 \rightarrow S_1$ $H \rightarrow L$ (99.58%)
			525.73	2.36	0.40	2.63	$S_0 \rightarrow S_2$ $H-1 \rightarrow L$ (96.57%)
			432.85	2.86	0.17	1.56	$S_0 \rightarrow S_4$ $H \rightarrow L+1$ (95.79%)
			350.42	3.54	0.17	1.38	$S_0 \rightarrow S_8$ $H-4 \rightarrow L$ (57.92%)
							$H-1 \rightarrow L+1$ (12.56%)
							$H \rightarrow L+3$ (13.21%)

Table S4. Fluorescence properties including maximum emission peaks (λ_{em}), oscillator strengths (f), fluorescence lifetimes (τ) and transition nature of the all molecules calculated by TDDFT method in water. The emission wavelengths (λ_{em}^{Exp}) are experimental results¹¹.

Molecules	B3LYP/6-311+G(d)				
	λ_{em}^{Exp}/nm	λ_{em}/nm	<i>f</i>	τ/ns^{-1}	Transition nature
DCCA	472	443.55	0.92	3.21	$S_1 \rightarrow S_0$ $H \rightarrow L$ (98.91%)
2		582.21	0.74	6.83	$S_1 \rightarrow S_0$ $H \rightarrow L$ (97.96%)
3		527.29	0.93	4.46	$S_1 \rightarrow S_0$ $H \rightarrow L$ (98.80%)
4		637.64	0.28	21.88	$S_1 \rightarrow S_0$ $H \rightarrow L$ (99.59%)
BC	693	659.86	1.34	4.86	$S_1 \rightarrow S_0$ $H \rightarrow L$ (98.91%)
BC-2		771.99	1.37	6.54	$S_1 \rightarrow S_0$ $H \rightarrow L$ (98.20%)

BC-3	753.00	1.37	6.20	$S_1 \rightarrow S_0$	H \rightarrow L	(97.91%)
BC-4	858.85	0.39	28.38	$S_1 \rightarrow S_0$	H \rightarrow L	(98.92%)

Table S5. Calculated the maximum two-photon absorption cross sections (σ_{max}) and corresponding TPA wavelengths (λ_{max}), at the ground-state geometries of experimental molecules^{11, 12} (DCCA and CMg1) by TD-DFT /6-311+G (d) methods, using different functionals

molecule	functional	B3LYP	BHandHLYP	CAM-B3LYP	Experimental data
DCCA	HF%	20	50	19, 65	
	λ_{max}/nm	792	693	725	760
	σ_{max}/GM	90.6	118.2	123.2	164.7
CMg1	λ_{max}/nm	932			820
	σ_{max}/GM	286			290

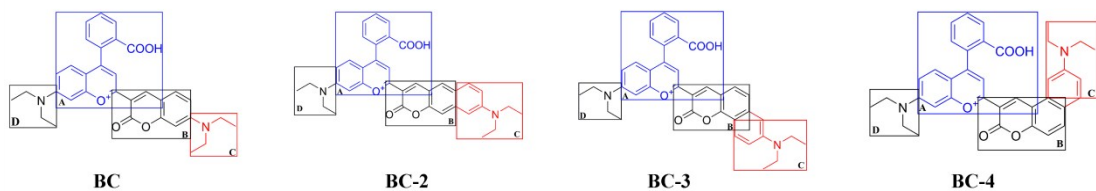


Fig.S6. Structures of fluorescent probe molecules and the divided regions for NBO analysis

Table S6. Natural atomic orbital occupancies analysis for fluorescent probe molecules. The subscripts 0 and 1 are for the ground state and the first excited state respectively. Δ represents the charge difference between above two electronic states.

Molecules	A ₀	A ₁	ΔA	B ₀	B ₁	ΔB	C ₀	C ₁	ΔC	D ₀	D ₁	ΔD
BC	0.67	0.46	-0.21	0.07	0.16	0.08	0.13	0.21	0.08	0.13	0.18	0.05
BC-2	0.68	0.41	-0.27	-0.15	-0.12	0.04	0.33	0.57	0.24	0.14	0.13	-0.01
BC-3	0.68	0.40	-0.29	-0.16	-0.11	0.06	0.34	0.58	0.24	0.14	0.13	-0.01
BC-4	0.70	0.38	-0.32	-0.13	-0.13	0.00	0.29	0.64	0.36	0.14	0.11	-0.03

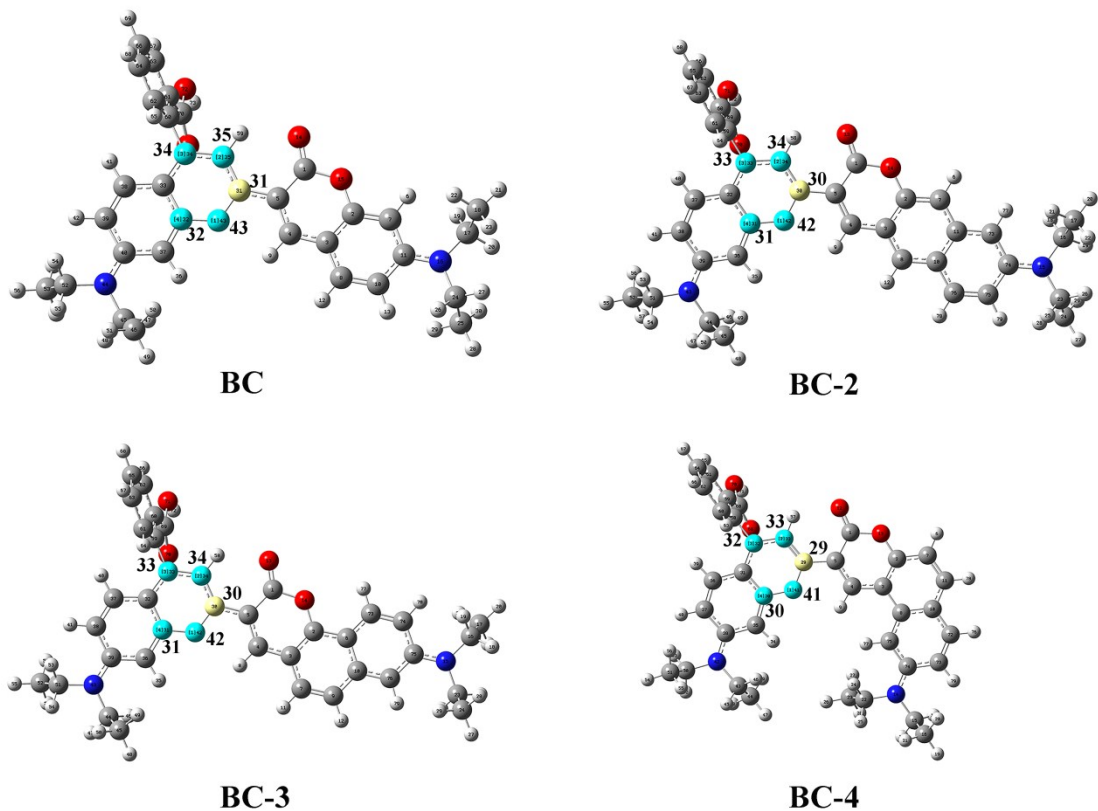


Fig.S7. Molecular structures and reactive site atoms for fluorescent probe molecules

Table S7. NBO analysis for fluorescent probe molecules at the ground state S0 and the first excited state S1. Δ represents the charge difference between above two electronic states.

Molecules	Atoms	S0	S1	Δ
BC	C31	0.43321	0.33512	-0.09809
	C32	0.39103	0.37069	-0.02034
	C33	-0.13342	-0.09582	0.0376
	C34	0.10219	-0.00159	-0.10378
	C35	-0.28843	-0.2172	0.07123
	C43	-0.44489	-0.47129	-0.0264
BC-2	C30	0.42976	0.34209	-0.08767
	C31	0.39228	0.37666	-0.01562
	C32	-0.13031	-0.1143	0.01601
	C33	0.10386	0.0136	-0.09026
	C34	-0.28425	-0.23997	0.04428
	C42	-0.44372	-0.46941	-0.02569
BC-3	C30	0.43068	0.33676	-0.09392
	C31	0.39208	0.375	-0.01708
	C32	-0.1311	-0.11285	0.01825
	C33	0.10377	0.0064	-0.09737
	C34	-0.28514	-0.23674	0.0484
	C42	-0.4432	-0.47082	-0.02762
BC-4	C29	0.43063	0.34408	-0.08655

C30	0.39268	0.37732	-0.01536
C31	-0.1288	-0.12323	0.00557
C32	0.10636	0.01604	-0.09032
C33	-0.28423	-0.25225	0.03198
C41	-0.44298	-0.47057	-0.02759

Notes and References

- 1 Niu, Y. L.; Peng, Q. A.; Deng, C. M.; Gao, X.; Shuai, Z. G., *J Phys Chem A* **2010**, *114* (30), 7817-7831.
- 2 Santoro, F.; Lami, A.; Imrota, R.; Bloino, J.; Barone, V., *J Chem Phys* **2008**, *128* (22), 224311.
- 3 Niu, Y.; Peng, Q.; Shuai, Z., *Science in China Series B: Chemistry* **2008**, *51* (12), 1153-1158.
- 4 Englman, R.; Jortner, J., *Molecular Physics* **1970**, *18* (2), 145-164.
- 5 Lin, S. H., *The Journal of Chemical Physics* **1966**, *44* (10), 3759-3767.
- 6 (a) Peticolas, W. L., *Annual Review of Physical Chemistry* **1967**, *18*(1), 233–260; (b) Beerepoot, M. T.; Friese, D. H.; List, N. H.; Kongsted, J.; Ruud, K., *Physical chemistry chemical physics* **2015**, *17* (29), 19306-14.
- 7 Rudberg, E.; Salek, P.; Helgaker, T.; Agren, H., *J Chem Phys* **2005**, *123* (18), 184108.
- 8 (a) Monson, P. R.; McClain, W. M., *The Journal of Chemical Physics* **1970**, *53* (1), 29-37; (b) Friese, D. H.; Beerepoot, M. T.; Ruud, K., *J Chem Phys* **2014**, *141* (20), 204103.
- 9 Aidas, K.; Angeli, C.; Bak, K. L.; Bakken, V.; Bast, R.; Boman, L.; Christiansen, O.; Cimiraglia, R.; Coriani, S.; Dahle, P.; Dalskov, E. K.; Ekstrom, U.; Enevoldsen, T.; Eriksen, J. J.; Ettenhuber, P.; Fernandez, B.; Ferrighi, L.; Fliegl, H.; Frediani, L.; Hald, K.; Halkier, A.; Hattig, C.; Heiberg, H.; Helgaker, T.; Hennum, A. C.; Hettema, H.; Hjertenaes, E.; Host, S.; Hoyvik, I. M.; Iozzi, M. F.; Jansik, B.; Jensen, H. J.; Jonsson, D.; Jorgensen, P.; Kauczor, J.; Kirpekar, S.; Kjaergaard, T.; Klopper, W.; Knecht, S.; Kobayashi, R.; Koch, H.; Kongsted, J.; Krapp, A.; Kristensen, K.; Ligabue, A.; Lutnaes, O. B.; Melo, J. I.; Mikkelsen, K. V.; Myhre, R. H.; Neiss, C.; Nielsen, C. B.; Norman, P.; Olsen, J.; Olsen, J. M.; Osted, A.; Packer, M. J.; Pawlowski, F.; Pedersen, T. B.; Provasi, P. F.; Reine, S.; Rinkevicius, Z.; Ruden, T. A.; Ruud, K.; Rybkin, V. V.; Salek, P.; Samson, C. C.; de Meras, A. S.; Saue, T.; Sauer, S. P.; Schimmelpfennig, B.; Sneskov, K.; Steindal, A. H.; Sylvester-Hvid, K. O.; Taylor, P. R.; Teale, A. M.; Tellgren, E. I.; Tew, D. P.; Thorvaldsen, A. J.; Thogersen, L.; Vahtras, O.; Watson, M. A.; Wilson, D. J.; Ziolkowski, M.; Agren, H., *Wiley interdisciplinary reviews. Computational molecular science* **2014**, *4* (3), 269-284.
- 10 Kim, I.; Kim, D.; Sambasivan, S.; Ahn, K. H., *Asian Journal of Organic Chemistry* **2012**, *1* (1), 60-64.
- 11 Dong, B.; Song, X.; Kong, X.; Wang, C.; Tang, Y.; Liu, Y.; Lin, W., *Adv. Mater.* **2016**, *28* (39), 8755-8759.
- 12 Kim, H. M.; Yang, P. R.; Seo, M. S.; Yi, J. S.; Hong, J. H.; Jeon, S. J.; Ko, Y. G.; Lee, K. J.; Cho, B. R., *J. Org. Chem.* **2007**, *72* (6), 2088-2096.